Decentralized Optimal Dispatch of Photovoltaic Inverters in Residential Distribution Systems

Emiliano Dall'Anese, *Member, IEEE*, Sairaj V. Dhople, *Member, IEEE*, Brian B. Johnson, *Member, IEEE*, and Georgios B. Giannakis, *Fellow, IEEE*

***Abstract*—Decentralized methods for computing optimal real and reactive power setpoints for residential photovoltaic (PV) inverters are developed in this paper. It is known that conventional PV inverter controllers, which are designed to extract maximum power at unity power factor, cannot address secondary performance objectives such as voltage regulation and network loss minimization. Optimal power flow techniques can be utilized to select which inverters will provide ancillary services and to compute their optimal real and reactive power setpoints according to well-defined performance criteria and economic objectives. Leveraging advances in sparsity-promoting regularization techniques and semidefinite relaxation, this paper shows how such problems can be solved with reduced computational burden and optimality guarantees. To enable large-scale implementation, a novel algorithmic framework is introduced—based on the so-called alternating direction method of multipliers—by which optimal power flow-type problems in this setting can be systematically decomposed into subproblems that can be solved in a decentralized fashion by the utility and customer-owned PV systems with limited exchanges of information. Since the computational burden is shared among multiple devices and the requirement of all-to-all communication can be circumvented, the proposed optimization approach scales favorably to large distribution networks.**

***Index Terms*—Alternating direction method of multipliers (ADMM), decentralized optimization, distribution systems, optimal power flow (OPF), photovoltaic systems, sparsity, voltage regulation.**

I. Introduction

THE PROLIFERATION of residential-scale photovoltaic (PV) systems has highlighted unique challenges and concerns in the operation and control of low-voltage distribution networks. Secondary-level control of PV inverters can alleviate extenuating circumstances such as overvoltages during periods when PV generation exceeds the household demand and voltage transients during rapidly varying atmospheric conditions [1]. Initiatives to upgrade inverter controls and develop business models for ancillary services are currently underway in order to facilitate large-scale integration of renewables while ensuring reliable operation of existing distribution feeders [2].

Examples of ancillary services include reactive power compensation, which has been recognized as a viable option to effect voltage regulation at the medium-voltage distribution level [3]–[7]. The amount of reactive power injected or absorbed by inverters can be computed based on either local droop-type proportional laws [3], [5] or optimal power flow (OPF) strategies [6], [7]. Either way, voltage regulation with this approach comes at the expense of low power factors at the substation and high network currents, with the latter leading to high power losses in the network [8]. Alternative approaches require inverters to operate at unity power factor and to curtail part of the available active power [8], [9]. For instance, heuristics based on droop-type laws are developed in [8] to compute the active power curtailed by each inverter in a residential system. Active power curtailment (APC) strategies are particularly effective in the low-voltage portion of distribution feeders, where the high resistance-to-inductance ratio of low-voltage overhead lines renders voltage magnitudes more sensitive to variations in the active power injections [10].

Recently, we proposed an optimal inverter dispatch (OID) framework [11], where the subset of critical PV inverters that most strongly impact network performance objectives are identified, and their real and reactive power setpoints are computed. This is accomplished by formulating an OPF-type problem, which encapsulates well-defined performance criteria as well as network and inverter operational constraints. By leveraging advances in sparsity-promoting regularizations and semidefinite relaxation (SDR) techniques [11], the problem is then solved by a centralized computational device with reduced computational burden. The proposed OID framework provides increased flexibility over Volt/Volt-Ampere Reactive (VAR) approaches [3], [5]–[7] and APC methods [8], [9] by: 1) determining in real time those inverters that must participate in ancillary services provisioning; and 2) jointly optimizing both the real and reactive power produced by the participating inverters (see, e.g., Fig. 3(c) and (d) for an illustration of the inverters' operating regions under OID).

As proposed originally, the OID task can be carried out on a centralized computational device which has to communicate with all inverters. In this paper, the OID problem proposed in [11] is strategically decomposed into subproblems that can be solved in a decentralized fashion by the utility-owned energy managers and customer-owned PV systems, with limited exchanges of information. Hereafter, this suite of decentralized

Manuscript received March 5, 2014; revised July 23, 2014; accepted September 4, 2014. Date of publication October 13, 2014; date of current version November 20, 2014. This work was supported by National Science Foundation-Computing and Communication Foundations (NSF-CCF) under Grant 1423316 and Grant CyberSEES 1442686; by the Institute of Renewable Energy and the Environment, University of Minnesota, under Grant RL-0010-13; and by the Laboratory Directed Research and Development Program at the National Renewable Energy Laboratory. Paper no. TEC-00174-2014.

E. Dall'Anese, S. V. Dhople, and G. B. Giannakis are with the Department of Electrical and Computer Engineering and Digital Technology Center, University of Minnesota, Minneapolis, MN 55455 USA (e-mail: emiliano@umn.edu; sdhople@umn.edu; georgios@umn.edu).

B. B. Johnson is with the National Renewable Energy Laboratory, Golden, CO 80401 USA (e-mail: brian.johnson@nrel.gov).

Color versions of one or more of the figures in this paper are available online at http://ieeexplore.ieee.org.

Digital Object Identifier 10.1109/TEC.2014.2357997

optimization algorithms is referred to as *decentralized optimal inverter dispatch* (DOID). Building on the concept of leveraging both real and reactive power optimization [11], and decentralized solution approaches for OPF problems [12], two novel decentralized approaches are developed in this paper. In the first setup, all customer-owned PV inverters can communicate with the utility. The utility optimizes network performance (quantified in terms of, e.g., power losses and voltage regulation) while individual customers maximize their economic objectives (quantified in terms of, e.g., the amount of active power they might have to curtail). This setup provides flexibility to the customers to specify their optimization objectives since the utility has no control on customer preferences. In the spirit of the advanced metering infrastructure paradigm, utility- and customer-owned energy manager units (EMUs) exchange relevant information [13], [14] to *agree* on the optimal PV inverter setpoints. Once the decentralized algorithms have converged, the active and reactive setpoints are implemented by the inverter controllers. In the second DOID approach, the distribution network is partitioned into *clusters*, each of which contains a set of customer-owned PV inverters and a single cluster energy manager (CEM). A decentralized algorithm is then formulated such that the operation of each cluster is optimized, and with a limited exchange of voltage-related messages, the interconnected clusters consent on the system-wide voltage profile. The DOID frameworks are developed by leveraging the alternating direction method of multipliers (ADMM) [15], [16].

Related works include [17], where augmented Lagrangian methods (related to ADMM) were employed to decompose nonconvex OPF problems for transmission systems into per-area instances, and [18], [19], where standard Lagrangian approaches were utilized in conjunction with Newton methods. ADMM was utilized in [20] to solve nonconvex OPF renditions in a decentralized fashion, and in [21], where successive convex approximation methods were utilized to deal with nonconvex costs and constraints. In the distribution systems context, SDRs of the OPF problem for balanced systems were developed in [22] and solved via node-to-node message passing by using dual (sub-)gradient ascent-based schemes. Similar message passing is involved in the ADMM-based decentralized algorithm proposed in [4], where a reactive power compensation problem based on approximate power flow models is solved. SDR of the OPF task in three-phase unbalanced systems was developed in [12]; the resultant semidefinite program was solved in a distributed fashion by using ADMM.

The DOID framework considerably broadens the setups of [12] and [17]–[22] by accommodating different message-passing strategies that are relevant in a variety of practical scenarios (e.g., customer-to-utility, customer-to-CEM, and CEM-to-CEM communications). The proposed decentralized schemes offer improved optimality guarantees over [17]–[20], since it is grounded on an SDR technique; furthermore, ADMM enables superior convergence compared to [22]. Finally, different from the distributed reactive compensation strategy of [4], the proposed framework considers the utilization of an exact ac power flow model, as well as a joint computation of active and reactive power setpoints.

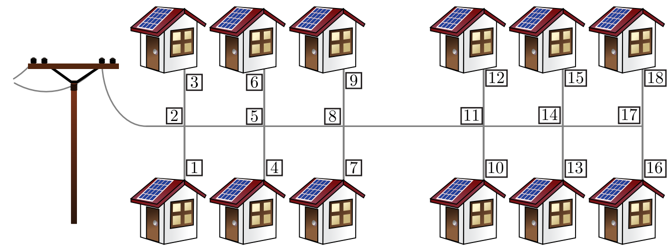

Fig. 1. Example of low-voltage residential network with high PV penetration, utilized in the test cases discussed in Section V. Node 0 corresponds to the secondary of the step-down transformer; set $\mathcal{U} = \{2, 5, 8, 11, 14, 17\}$ collects nodes corresponding to distribution poles; and homes $\mathrm{H}_1, \ldots, \mathrm{H}_{12}$ are connected to nodes in the set $\mathcal{H} = \{1, 3, 4, 6, 7, 9, 10, 12, 13, 15, 16, 18\}$.

For completeness, ADMM was utilized also in [23] and [24] for decentralized multiarea state estimation in transmission systems, and in [25] to distribute over geographical areas the distribution system reconfiguration task.

The remainder of this paper is organized as follows. Section II briefly outlines the centralized OID problem proposed in [11]. Sections III and IV describe the two DOID problems discussed above. Case studies to validate the approach are presented in Section V. Finally, concluding remarks and directions for future work are presented in Section VI.

Notation: Uppercase (lowercase) boldface letters will be used for matrices (column vectors); $(\cdot)^{\mathsf{T}}$ for transposition; $(\cdot)^*$ complex-conjugate; and $(\cdot)^{\mathsf{H}}$ complex-conjugate transposition; $\Re\{\cdot\}$ and $\Im\{\cdot\}$ denote the real and imaginary parts of a complex number, respectively; $\mathrm{j} := \sqrt{-1}$ the imaginary unit. $\mathrm{Tr}(\cdot)$ the matrix trace; $\mathrm{rank}(\cdot)$ the matrix rank; $|\cdot|$ denotes the magnitude of a number or the cardinality of a set; $\|\mathbf{v}\|_2 := \sqrt{\mathbf{v}^{\mathsf{H}}\mathbf{v}}$; $\|\mathbf{v}\|_1 := \sum_i |[\mathbf{v}]_i|$; and $\|\cdot\|_F$ stands for the Frobenius norm. Given a given matrix $\mathbf{X}$, $[\mathbf{X}]_{m,n}$ denotes its (m, n)th entry. Finally, $\mathbf{I}_N$ denotes the $N \times N$ identity matrix; and $\mathbf{0}_{M\times N}$, $\mathbf{1}_{M\times N}$ the $M \times N$ matrices with all zeroes and ones, respectively.

II. Centralized OID

A. Network and PV Inverter Models

Consider a distribution system comprising $N + 1$ nodes collected in the set $\mathcal{N} := \{0, 1, \ldots, N\}$ (node 0 denotes the secondary of the step-down transformer), and lines represented by the set of edges $\mathcal{E} := \{(m, n)\} \subset \mathcal{N} \times \mathcal{N}$. For simplicity of exposition, a balanced system is considered; however, both the centralized and decentralized frameworks proposed subsequently can be extended to unbalanced systems following the methods in [12]. Subsets $\mathcal{U}, \mathcal{H} \subset \mathcal{N}$ collect nodes corresponding to utility poles (with zero power injected or consumed), and those with installed residential PV inverters, respectively (see Fig. 1).

Let $V_n \in \mathbb{C}$ and $I_n \in \mathbb{C}$ denote the phasors for the line-to-ground voltage and the current injected at node $n \in \mathcal{N}$, respectively, and define $\mathbf{i} := [I_1, \ldots, I_N]^{\mathsf{T}} \in \mathbb{C}^N$ and $\mathbf{v} := [V_1, \ldots, V_N]^{\mathsf{T}} \in \mathbb{C}^N$. Using Ohm's and Kirchhoff's circuit laws, the linear relationship $\mathbf{i} = \mathbf{Y}\mathbf{v}$ can be established, where the system admittance matrix $\mathbf{Y} \in \mathbb{C}^{N+1\times N+1}$ is formed based

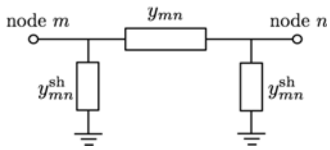

Fig. 2. π-equivalent circuits of a low-voltage distribution line $(m,n) \in \mathcal{E}$.

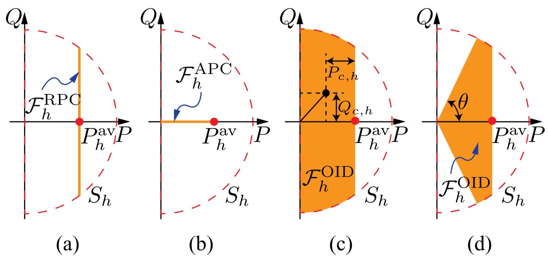

Fig. 3. Feasible operating regions for the hth inverter with apparent power rating S_h under (a) reactive power control, (b) APC, (c) OID with joint control of real and reactive power, and (d) OID with a lower bound on power factor.

on the system topology and the π-equivalent circuit of lines $(m,n) \in \mathcal{E}$, as illustrated in Fig. 2; see also [10, Ch. 6] for additional details on line modeling. Specifically, with y_{mn} and $y^{\rm sh}_{mn}$ denoting the series and shunt admittances of line (m,n), the entries of $\mathbf{Y}$ are defined as

$$[\mathbf{Y}]_{m,n} := \begin{cases} \sum_{j \in \mathcal{N}_m} y^{\rm sh}_{mj} + y_{mj}, & \text{if } m = n \\ -y_{mn}, & \text{if } (m,n) \in \mathcal{E} \\ 0, & \text{otherwise} \end{cases}$$

where $\mathcal{N}_m := \{j \in \mathcal{N} : (m,j) \in \mathcal{E}\}$ denotes the set of nodes connected to the mth one through a distribution line.

A constant PQ model [10] is adopted for the load, with $P_{\ell,h}$ and $Q_{\ell,h}$ denoting the active and reactive demands at node $h \in \mathcal{H}$, respectively. For given solar irradiation conditions, let $P_h^{\rm av}$ denote the maximum *available active power* from the PV array at node $h \in \mathcal{H}$. The proposed framework calls for the joint control of *both* real and reactive power produced by the PV inverters. In particular, the allowed operating regime on the complex-power plane for the PV inverters is illustrated in Fig. 3(d) and described by

$$\mathcal{F}_h^{\rm OID} := \left\{ P_{c,h}, Q_{c,h} : \begin{array}{c} 0 \leq P_{c,h} \leq P_h^{\rm av} \\ Q_{c,h}^2 \leq S_h^2 - (P_h^{\rm av} - P_{c,h})^2 \\ |Q_{c,h}| \leq \tan\theta (P_h^{\rm av} - P_{c,h}) \end{array} \right\} \quad (1)$$

where $P_{c,h}$ is the active power curtailed, and $Q_{c,h}$ is the reactive power injected/absorbed by the inverter at node h. Notice that if there is no limit to the power factor, then $\theta = \pi/2$, and the operating region is given by Fig. 3(c).

B. Centralized Optimization Strategy

The centralized OID framework in [11] invokes joint optimization of active and reactive powers generated by the PV inverters, and it offers the flexibility of selecting the subset of critical PV inverters that should be dispatched in order to fulfill optimization objectives and ensure electrical network constraints. To this end, let z_h be a binary variable indicating whether PV inverter h provides ancillary services or not and assume that at most $K < |\mathcal{H}|$ PV inverters are allowed to provide ancillary services. Selecting a (possibly time-varying) subset of inverters promotes user fairness [3], prolongs inverter lifetime [3], and captures possible fixed-rate utility-customer pricing/rewarding strategies [2]. Let $\mathbf{p}_c$ and $\mathbf{q}_c$ collect the active powers curtailed and the reactive powers injected/absorbed by the inverters. With these definitions, the OID problem is formulated as follows:

$$\min_{\mathbf{v}, \mathbf{i}, \mathbf{p}_c, \mathbf{q}_c, \{z_h\}} \quad C(\mathbf{V}, \mathbf{p}_c) \quad (2a)$$

$$\text{subject to } \mathbf{i} = \mathbf{Y}\mathbf{v}, \ \{z_h\} \in \{0,1\}^{|\mathcal{H}|}, \text{ and}$$

$$V_h I_h^* = (P_h^{\rm av} - P_{c,h} - P_{\ell,h}) + \mathrm{j}(Q_{c,h} - Q_{\ell,h}) \quad (2b)$$

$$V_n I_n^* = 0 \qquad \forall n \in \mathcal{U} \quad (2c)$$

$$V^{\min} \leq |V_n| \leq V^{\max} \qquad \forall n \in \mathcal{N} \quad (2d)$$

$$(P_{c,h}, Q_{c,h}) \in \begin{cases} \{(0,0)\}, & \text{if } z_h = 0 \\ \mathcal{F}_h^{\rm OID}, & \text{if } z_h = 1 \end{cases} \qquad \forall h \in \mathcal{H} \quad (2e)$$

$$\sum_{h \in \mathcal{H}} z_h \leq K, \quad (2f)$$

where constraint (2b) is enforced at each node $h \in \mathcal{H}$; $C(\mathbf{V}, \mathbf{p}_c)$ is a given cost function capturing both network- and customer-oriented objectives [2], [11]; and (2e) and (2f) jointly indicate which inverters have to operate either under OID (i.e., $(P_{c,h}, Q_{c,h}) \in \mathcal{F}_h^{\rm OID}$), or, in the business-as-usual mode (i.e., $(P_{c,h}, Q_{c,h}) = (0,0)$). An alternative problem formulation can be obtained by removing constraint (2f), and adopting the cost $C(\mathbf{V}, \mathbf{p}_c) + \lambda_z \sum_{h \in \mathcal{H}} z_h$ in (2a), with $\lambda_z \geq 0$ a weighting coefficient utilized to tradeoff achievable cost $C(\mathbf{V}, \mathbf{p}_c)$ for the number of controlled inverters. When λ_z represents a fixed reward for customers providing ancillary services [2] and $C(\mathbf{V}, \mathbf{p}_c)$ models costs associated with active power losses and active power setpoints, OID (2a) returns the inverter setpoints that minimize the economic cost incurred by feeder operation.

As with various OPF-type problem formulations, the power balance and lower bound on the voltage magnitude constraints (2b), (2c) and (2d), respectively, render the OID problem nonconvex, and thus challenging to solve optimally and efficiently. Unique to the OID formulation are the binary optimization variables $\{z_h\}$; finding the optimal (sub)set of inverters to dispatch involves the solution of combinatorially many subproblems. Nevertheless, a computationally affordable *convex* reformulation was developed in [11], by leveraging sparsity-promoting regularization [26] and SDR techniques [12], [23], [27], as briefly described next.

In order to bypass binary selection variables, key is to notice that that if inverter h is *not* selected for ancillary services, then one clearly has that $P_{c,h} = Q_{c,h} = 0$ [cf., (2e)]. Thus, for $K < |\mathcal{H}|$, one has that the $2|\mathcal{H}| \times 1$ real-valued vector $[P_{c,1}, Q_{c,1}, \ldots, P_{c,|\mathcal{H}|}, Q_{c,|\mathcal{H}|}]^{\mathsf{T}}$ is *group sparse* [26]; meaning that, either the 2×1 subvectors $[P_{c,h}, Q_{c,h}]^\mathsf{T}$ equal $\mathbf{0}$ or not [11]. This group-sparsity attribute enables discarding the binary variables and to effect PV inverter selection by regularizing the cost in (2a) with the following function:

$$G(\mathbf{p}_c, \mathbf{q}_c) := \lambda \sum_{h \in \mathcal{H}} \|[P_{c,h}, Q_{c,h}]^\mathrm{T}\|_2 \tag{3}$$

where $\lambda \geq 0$ is a tuning parameter. Specifically, the number of inverters operating under OID decreases as λ is increased [26].

Key to developing a relaxation of the OID task is to express powers and voltage magnitudes as linear functions of the outer-product Hermitian matrix $\mathbf{V} := \mathbf{v}\mathbf{v}^\mathsf{H}$, and to reformulate the OID problem with cost and constraints that are linear in $\mathbf{V}$, as well as the constraints $\mathbf{V} \succeq \mathbf{0}$ and $\mathrm{rank}(\mathbf{V}) = 1$ [12], [23], [27]. The resultant problem is still nonconvex because of the constraint $\mathrm{rank}(\mathbf{V}) = 1$; however, in the spirit of SDR, this constraint can be dropped.

To this end, define the matrix $\mathbf{Y}_n := \mathbf{e}_n \mathbf{e}_n^\mathsf{T} \mathbf{Y}$ per node n, where $\{\mathbf{e}_n\}_{n \in \mathcal{N}}$ denotes the canonical basis of $\mathbb{R}^{|\mathcal{N}|}$. Based on $\mathbf{Y}_n$, define also the Hermitian matrices $\mathbf{A}_n := \frac{1}{2}(\mathbf{Y}_n + \mathbf{Y}_n^\mathsf{H})$, $\mathbf{B}_n := \frac{j}{2}(\mathbf{Y}_n - \mathbf{Y}_n^\mathsf{H})$, and $\mathbf{M}_n := \mathbf{e}_n \mathbf{e}_n^\mathsf{T}$. Using these matrices, along with (3), the relaxed convex OID problem can be formulated as

$$\begin{aligned}
\min_{\mathbf{V},\, \mathbf{p}_c,\, \mathbf{q}_c} \quad & C(\mathbf{V},\, \mathbf{p}_c) + G(\mathbf{p}_c,\, \mathbf{q}_c) && && \text{(4a)}\\
\text{s.to } \mathbf{V} \succeq {} & \mathbf{0}, \text{ and} && && \\
\mathrm{Tr}(\mathbf{A}_h \mathbf{V}) = {} & -P_{\ell,h} + P_h^{\mathrm{av}} - P_{c,h} && \forall h \in \mathcal{H} && \text{(4b)}\\
\mathrm{Tr}(\mathbf{B}_h \mathbf{V}) = {} & -Q_{\ell,h} + Q_{c,h} && \forall h \in \mathcal{H} && \text{(4c)}\\
\mathrm{Tr}(\mathbf{A}_n \mathbf{V}) = {} & 0, \mathrm{Tr}(\mathbf{B}_n \mathbf{V}) = 0 && \forall n \in \mathcal{U} && \text{(4d)}\\
V_{\min}^2 \leq {} & \mathrm{Tr}(\mathbf{M}_n \mathbf{V}) \leq V_{\max}^2 && \forall n \in \mathcal{N} && \text{(4e)}\\
(P_{c,h},\, Q_{c,h}) \in {} & \mathcal{F}_h^{\mathrm{OID}} && \forall h \in \mathcal{H}. && \text{(4f)}
\end{aligned}$$

If the optimal solution of the relaxed problem (4) has rank 1, then the resultant voltages, currents, and power flows are globally optimal for given inverter setpoints [27]. Sufficient conditions for SDR to be successful in OPF-type problems are available for networks that are radial and balanced in [22] and [28], whereas the virtues of SDR for unbalanced medium- and low-voltage distribution systems have been demonstrated in [12]. As for the inverter setpoints $\{(P_h^{\mathrm{av}} - P_{c,h},\, Q_{c,h})\}$, those obtained from (4) may be slightly suboptimal compared to the setpoints that would have been obtained by solving the optimization problem (2). This is mainly due to the so-called shrinkage effect introduced by the regularizer (3) [26]. Unfortunately, a numerical assessment of the optimality gap is impractical, since finding the globally optimal solution of problem (2) under all setups is computationally infeasible.

To solve the OID problem, all customers' loads and available powers $\{P_h^{\mathrm{av}}\}$ must be gathered at a central processing unit (managed by the utility company), which subsequently dispatches the PV inverter setpoints. Next, decentralized implementations of the OID framework are presented so that the OID problem can be solved in a decentralized fashion with limited exchange of information. From a computational perspective, decentralized schemes ensure scalability of problem complexity with respect to the system size.

III. DOID: Utility-Customer Message Passing

Consider decoupling the cost $C(\mathbf{V}, \mathbf{p}_c)$ in (4a) as $C(\mathbf{V},\, \mathbf{p}_c) = C_{\mathrm{utility}}(\mathbf{V},\, \mathbf{p}_c) + \sum_h R_h(P_{c,h})$, where $C_{\mathrm{utility}}(\mathbf{V},\, \mathbf{p}_c)$ captures utility-oriented optimization objectives, which may include, e.g., power losses in the network and voltage deviations [6], [7], [11]; and $R_h(P_{c,h})$ is a convex function modeling the cost incurred by (or the reward associated with) customer h when the PV inverter is required to curtail power. Without loss of generality, a quadratic function $R_h(P_{c,h}) := a_h P_{c,h}^2 + b_h P_{c,h}$ is adopted here, where the choice of the coefficients is based on specific utility-customer prearrangements [2] or customer preferences [11].

Suppose that customer h transmits to the utility company the net active power $\bar{P}_h := -P_{\ell,h} + P_h^{\mathrm{av}}$ and the reactive load $Q_{\ell,h}$; subsequently, customer and utility will agree on the PV inverter setpoint, based on the optimization objectives described by C_{utility} and $\{R_h\}$. To this end, let $\bar{P}_{c,h}$ and $\bar{Q}_{c,h}$ represent *copies* of $P_{c,h}$ and $Q_{c,h}$, respectively, at the utility. The corresponding $|\mathcal{H}| \times 1$ vectors that collect the copies of the inverter setpoints are denoted by $\bar{\mathbf{p}}_c$ and $\bar{\mathbf{q}}_c$, respectively. Then, using the additional optimization variables $\bar{\mathbf{p}}_c, \bar{\mathbf{q}}_c$, the relaxed OID problem (4) can be equivalently reformulated as

$$\begin{aligned}
\min_{\substack{\mathbf{V},\mathbf{p}_c,\mathbf{q}_c\\ \bar{\mathbf{p}}_c,\bar{\mathbf{q}}_c}} \quad & \bar{C}(\mathbf{V}, \bar{\mathbf{p}}_c, \bar{\mathbf{q}}_c) + \sum_{h \in \mathcal{H}} R_h(P_{c,h}) && && \text{(5a)}\\
\text{s.to } \mathbf{V} \succeq {} & \mathbf{0}, \text{ and} && && \\
\mathrm{Tr}(\mathbf{A}_h \mathbf{V}) = {} & \bar{P}_h - \bar{P}_{c,h} && \forall h \in \mathcal{H} && \text{(5b)}\\
\mathrm{Tr}(\mathbf{B}_h \mathbf{V}) = {} & -Q_{\ell,h} + \bar{Q}_{c,h} && \forall h \in \mathcal{H} && \text{(5c)}\\
\mathrm{Tr}(\mathbf{A}_n \mathbf{V}) = {} & 0, \mathrm{Tr}(\mathbf{B}_n \mathbf{V}) = 0 && \forall n \in \mathcal{U} && \text{(5d)}\\
V_{\min}^2 \leq {} & \mathrm{Tr}(\mathbf{M}_h \mathbf{V}) \leq V_{\max}^2 && \forall n \in \mathcal{N} && \text{(5e)}\\
(P_{c,h},\, Q_{c,h}) \in {} & \mathcal{F}_h^{\mathrm{OID}} && \forall h \in \mathcal{H} && \text{(5f)}\\
\bar{P}_{c,h} = {} & P_{c,h},\ \bar{Q}_{c,h} = Q_{c,h} && \forall h \in \mathcal{H} && \text{(5g)}
\end{aligned}$$

where constraints (5g) ensure that utility and customer *agree* upon the inverters' setpoints, and $\bar{C}(\mathbf{V},\, \bar{\mathbf{p}}_c,\, \bar{\mathbf{q}}_c) := C_{\mathrm{utility}}(\mathbf{V},\, \bar{\mathbf{p}}_c) + G(\bar{\mathbf{p}}_c,\, \bar{\mathbf{q}}_c)$ is the regularized cost function to be minimized at the utility.

The consensus constraints (5g) render problems (4) and (5) equivalent; however, the same constraints impede problem decomposability, and thus, modern optimization techniques such as distributed (sub-)gradient methods [13], [14], and ADMM [15, Sec. 3.4] cannot be directly applied to solve (5) in a decentralized fashion. To enable problem decomposability, consider introducing the auxiliary variables x_h, y_h per inverter h. Using these auxiliary variables, (5) can be reformulated as

$$\begin{aligned}
\min_{\substack{\mathbf{V},\mathbf{p}_c,\mathbf{q}_c\\ \bar{\mathbf{p}}_c,\bar{\mathbf{q}}_c,\{x_h,y_h\}}} \quad & \bar{C}(\mathbf{V}, \bar{\mathbf{p}}_c, \bar{\mathbf{q}}_c) + \sum_{h \in \mathcal{H}} R_h(P_{c,h}) && \text{(6a)}\\
\text{s.to } \mathbf{V} \succeq {} & \mathbf{0},\ \text{(5b)–(5f)},\ \text{and} && \\
\bar{P}_{c,h} = {} & x_h, \quad x_h = P_{c,h} \quad \forall h \in \mathcal{H} && \text{(6b)}\\
\bar{Q}_{c,h} = {} & y_h, \quad y_h = Q_{c,h} \quad \forall h \in \mathcal{H}. && \text{(6c)}
\end{aligned}$$

Problem (6) is equivalent to (4) and (5); however, compared to (4) and (5), it is amenable to a decentralized solution via ADMM [15, Sec. 3.4] as described in the remainder of this section. ADMM is preferred over distributed (sub-)gradient schemes because of its significantly faster convergence [4] and resilience to communication errors [29].

Per inverter h, let $\bar{\gamma}_h$ and γ_h denote the multipliers associated with the two constraints in (17c), and $\bar{\mu}_h, \mu_h$ the ones associated with (17d). Next, consider the partial quadratically augmented Lagrangian of (6a), defined as follows:

$$\begin{aligned}\mathcal{L}(\bar{\mathcal{P}}, \{\mathcal{P}_h\}, \mathcal{P}_{xy}, \mathcal{D}) := \bar{C}(\mathbf{V}, \bar{\mathbf{p}}_c, \bar{\mathbf{q}}_c) + \sum_{h\in\mathcal{H}} \Big[R_h(P_{c,h}) \\ + \bar{\gamma}_h(\bar{P}_{c,h} - x_h) + \gamma_h(x_h - P_{c,h}) + \bar{\mu}_h(\bar{Q}_{c,h} - y_h) \\ + \mu_h(y_h - Q_{c,h}) + (\kappa/2)(\bar{P}_{c,h} - x_h)^2 + (\kappa/2)(x_h - P_{c,h})^2 \\ + (\kappa/2)(\bar{Q}_{c,h} - y_h)^2 + (\kappa/2)(y_h - Q_{c,h})^2\Big] \end{aligned} \tag{7}$$

where $\bar{\mathcal{P}} := \{\mathbf{V}, \bar{\mathbf{p}}_c, \bar{\mathbf{q}}_c\}$ collects the optimization variables of the utility; $\mathcal{P}_h := \{P_{c,h}, Q_{c,h}\}$ are the decision variables for customer h; $\mathcal{P}_{xy} := \{x_h, y_h, \forall h \in \mathcal{H}\}$ is the set of auxiliary variables; $\mathcal{D} := \{\bar{\gamma}_h, \gamma_h, \bar{\mu}_h, \mu_h, \forall h \in \mathcal{H}\}$ collects the dual variables; and $\kappa > 0$ is a given constant. Based on (7), ADMM amounts to iteratively performing the steps **[S1]–[S3]** described next, where i denotes the iteration index:

[S1] Update variables $\bar{\mathcal{P}}$ as follows:

$$\bar{\mathcal{P}}[i+1] := \arg \min_{\mathbf{V}, \{\bar{P}_{c,h}, \bar{Q}_{s,h}\}} \mathcal{L}(\bar{\mathcal{P}}, \{\mathcal{P}_h[i]\}, \mathcal{P}_{xy}[i], \mathcal{D}[i]) \quad \text{s. to } \mathbf{V} \succeq \mathbf{0}, \text{ and } (5b)\text{–}(5e). \tag{8}$$

Furthermore, per inverter h, update $P_{c,h}, Q_{c,h}$ as follows:

$$\mathcal{P}_h[i+1] : = \arg \min_{P_{c,h}, Q_{c,h}} \mathcal{L}(\bar{\mathcal{P}}[i], P_{c,h}, Q_{c,h}, \mathcal{P}_{xy}[i], \mathcal{D}[i]) \quad \text{s. to } (P_{c,h}, Q_{c,h}) \in \mathcal{F}_h^{\text{OID}}. \tag{9}$$

[S2] Update auxiliary variables $\mathcal{P}_{xy}$:

$$\mathcal{P}_{xy}[i+1] := \arg \min_{\{x_h, y_h\}} \mathcal{L}(\bar{\mathcal{P}}[i+1], \{\mathcal{P}_h[i+1]\}, \{x_h, y_h\}, \mathcal{D}[i]). \tag{10}$$

[S3] Dual update:

$$\bar{\gamma}_h[i+1] = \bar{\gamma}_h[i] + \kappa(\bar{P}_{c,h}[i+1] - x_h[i+1]) \tag{11a}$$
$$\gamma_h[i+1] = \gamma_h[i] + \kappa(x_h[i+1] - P_{c,h}[i+1]) \tag{11b}$$
$$\bar{\mu}_h[i+1] = \bar{\mu}_h[i] + \kappa(\bar{Q}_{c,h}[i+1] - y_h[i+1]) \tag{11c}$$
$$\mu_h[i+1] = \mu_h[i] + \kappa(y_h[i+1] - Q_{c,h}[i+1]). \tag{11d}$$

In **[S1]**, the primal variables $\bar{\mathcal{P}}, \{\mathcal{P}_h\}$ are obtained by minimizing (7), where the auxiliary variables $\mathcal{P}_{xy}$ and the multipliers $\mathcal{D}$ are kept fixed to their current iteration values. Likewise, the auxiliary variables are updated in **[S2]** by fixing $\bar{\mathcal{P}}, \{\mathcal{P}_h\}$ to their up-to-date values. Finally, the dual variables are updated in **[S3]** via dual gradient ascent.

It can be noticed that step **[S2]** favorably decouples into $2|\mathcal{H}|$ scalar and unconstrained quadratic programs, with $x_h[i+1]$ and $y_h[i+1]$ solvable in closed form. Using this feature, the following lemma can be readily proved.

Lemma 1: Suppose that the multipliers are initialized as $\bar{\gamma}_h[0] = \gamma_h[0] = \bar{\mu}_h[0] = \mu_h[0] = 0$. Then, for all iterations $i > 0$, it holds that:

1) $\bar{\gamma}_h[i] = \gamma_h[i]$;
2) $\bar{\mu}_h[i] = \mu_h[i]$;
3) $x_h[i] = \frac{1}{2}\bar{P}_{c,h}[i] + \frac{1}{2}P_{c,h}[i]$;
4) $y_h[i] = \frac{1}{2}\bar{Q}_{c,h}[i] + \frac{1}{2}Q_{c,h}[i]$.

Using Lemma 1, the conventional ADMM steps **[S1]–[S3]** can be simplified as follows.

[S1′] At the utility side, variables $\bar{\mathcal{P}}$ are updated by solving the following convex optimization problem:

$$\begin{aligned}\bar{\mathcal{P}}[i+1] := \arg \min_{\mathbf{V}, \{\bar{P}_{c,h}, \bar{Q}_{s,h}\}} & \bar{C}(\mathbf{V}, \bar{\mathbf{p}}_c, \bar{\mathbf{q}}_c) \\ & + F(\bar{\mathbf{p}}_c, \bar{\mathbf{q}}_c, \{\mathcal{P}_h[i]\}) \\ & \text{s. to } \mathbf{V} \succeq \mathbf{0}, \text{ and } (5b)\text{–}(5e) \end{aligned} \tag{12a}$$

where function $F(\bar{\mathbf{p}}_c, \bar{\mathbf{q}}_c, \{\mathcal{P}_h[i]\})$ is defined as

$$\begin{aligned}F(\bar{\mathbf{p}}_c, \bar{\mathbf{q}}_c, \{\mathcal{P}_h[i]\}) := \sum_{h\in\mathcal{H}} \Big[& \frac{\kappa}{2}(\bar{P}_{c,h}^2 + \bar{Q}_{c,h}^2) \\ & + \bar{P}_{c,h}\left(\gamma_h[i] - \frac{\kappa}{2}\bar{P}_{c,h}[i] - \frac{\kappa}{2}P_{c,h}[i]\right) \\ & + \bar{Q}_{c,h}\left(\mu_h[i] - \frac{\kappa}{2}\bar{Q}_{c,h}[i] \right. \\ & \left. - \frac{\kappa}{2}Q_{c,h}[i]\right)\Big]. \end{aligned} \tag{12b}$$

At the customer side, the PV inverter setpoints are updated by solving the following constrained quadratic program:

$$\begin{aligned}\mathcal{P}_h[i+1] := \arg \min_{P_{c,h}, Q_{c,h}} \Big[& R_h(P_{c,h}) + \frac{\kappa}{2}\left(P_{c,h}^2 + Q_{c,h}^2\right) \\ & - P_{c,h}\left(\gamma_h[i] + \frac{\kappa}{2}\bar{P}_{c,h}[i] + \frac{\kappa}{2}P_{c,h}[i]\right) \\ & - Q_{c,h}\left(\mu_h[i] + \frac{\kappa}{2}\bar{Q}_{c,h}[i] + \frac{\kappa}{2}Q_{c,h}[i]\right)\Big] \\ & \text{s. to } (P_{c,h}, Q_{c,h}) \in \mathcal{F}_h^{\text{OID}}. \end{aligned} \tag{13}$$

[S2′] At the utility and customer sides, the dual variables are updated as

$$\gamma_h[i+1] = \gamma_h[i] + \frac{\kappa}{2}(\bar{P}_{c,h}[i+1] - P_{c,h}[i+1]) \tag{14a}$$
$$\mu_h[i+1] = \mu_h[i] + \frac{\kappa}{2}(\bar{Q}_{c,h}[i+1] - Q_{c,h}[i+1]). \tag{14b}$$

The resultant decentralized algorithm entails a two-way message exchange between the utility and customers of the current iterates $\bar{\mathbf{p}}_c[i], \bar{\mathbf{q}}_c[i]$ and $\mathbf{p}_c[i], \mathbf{q}_c[i]$. Specifically, at each iteration $i > 0$, the utility-owned device solves the OID rendition (12) to update the desired PV inverter setpoints based on the performance objectives described by $\bar{C}(\mathbf{V}, \bar{\mathbf{p}}_c, \bar{\mathbf{q}}_c)$ (which is

Algorithm 1 DOID: Utility-customer message passing.

Set $\gamma_h[0] = \mu_h[0] = 0$ for all $h \in \mathcal{H}$.
for $i = 1, 2, \ldots$ (repeat until convergence) **do**

1. **[Utility]**: update $\mathbf{V}[i+1]$ and $\{\bar{P}_{c,h}[i+1], \bar{Q}_{c,h}[i+1]\}$ via (12).
   [Customer-h]: update $\bar{P}_{c,h}[i+1], \bar{Q}_{c,h}[i+1]$ via (13).
2. **[Utility]**: send $\bar{P}_{c,h}[i+1], \bar{Q}_{c,h}[i+1]$ to h;
   repeat for all $h \in \mathcal{H}$.
   [Customer-h]: receive $\bar{P}_{c,h}[i+1], \bar{Q}_{c,h}[i+1]$ from utility;
   send $P_{c,h}[i+1], Q_{c,h}[i+1]$ to utility;
   repeat for all $h \in \mathcal{H}$.
   [Utility]: receive $P_{c,h}[i+1], Q_{c,h}[i+1]$ from h;
   repeat for all $h \in \mathcal{H}$.
3. **[Utility]**: update $\{\gamma_h[i+1], \mu_h[i+1]\}_{h\in\mathcal{H}}$ via (14).
   [Customer-h]: update dual variables $\gamma_h[i+1], \mu_h[i+1]$ via (14);
   repeat for all $h \in \mathcal{H}$.

end for
Implement setpoints in the PV inverters.

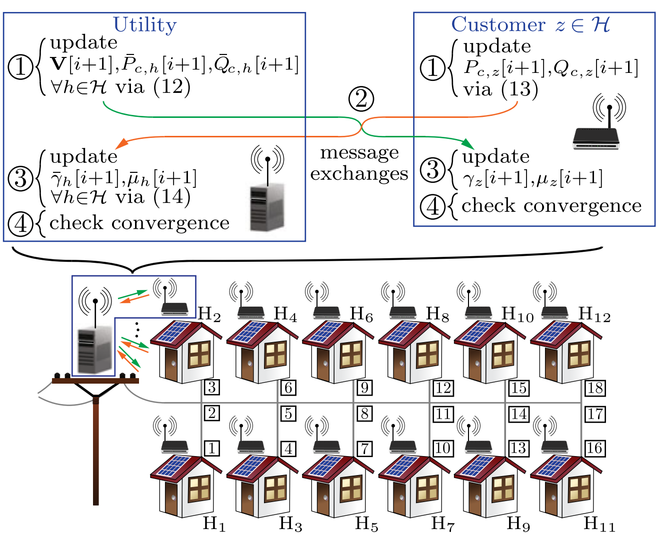

Fig. 4. DOID: scenario with utility-customer message passing according to Algorithm 1.

regularized with the term $F(\bar{\mathbf{p}}_c, \bar{\mathbf{q}}_c, \{\mathcal{P}_h[i]\})$ enforcing consensus with the setpoints computed at the customer side), as well as the electrical network constraints (5b)–(5e); once (12) is solved, the utility relays to each customer a copy of the iterate value $(\bar{P}_{c,h}[i+1], \bar{Q}_{c,h}[i+1])$. In the meantime, the PV inverter setpoints are simultaneously updated via (13) and subsequently sent to the utility. Once the updated local iterates are exchanged, utility and customers update the local dual variables (14).

The resultant decentralized algorithm is tabulated as Algorithm 1, illustrated in Fig. 4, and its convergence to the solution of the centralized OID problem (4a) is formally stated next.

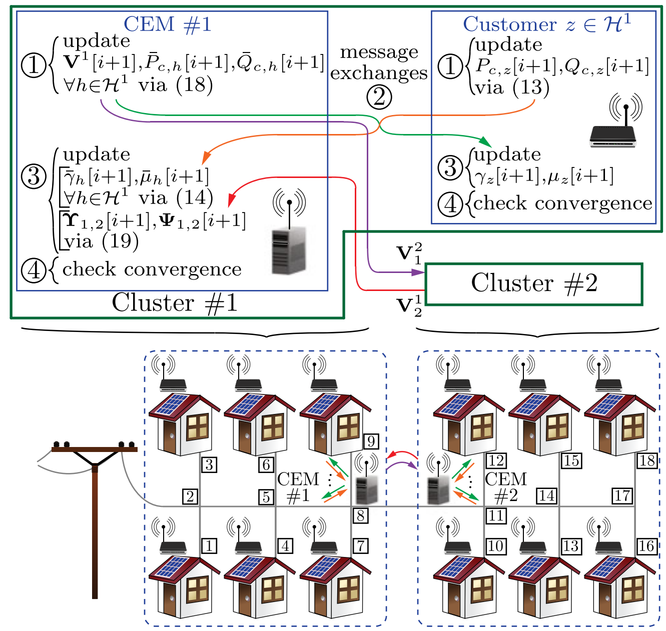

Fig. 5. Network division into clusters and illustration of Algorithm 2. In this setup, $\mathcal{C}^1 = \{1, \ldots, 9\}$, $\tilde{\mathcal{C}}^1 = \{1, \ldots, 9, 11\}$, $\mathcal{C}^2 = \{10, \ldots, 18\}$, and $\tilde{\mathcal{C}}^2 = \{8, 10, \ldots, 18\}$.

Proposition 1: The iterates $\bar{\mathcal{P}}[i], \{\mathcal{P}_h[i]\}$ and $\mathcal{D}[i]$ produced by **[S1′]–[S2′]** are convergent, for any $\kappa > 0$. Further, $\lim_{i\to+\infty} \mathbf{V}[i] = \mathbf{V}^{\text{opt}}$, $\lim_{i\to+\infty} \mathbf{p}_c[i] = \lim_{i\to+\infty} \bar{\mathbf{p}}_c[i] = \mathbf{p}_c^{\text{opt}}$ and $\lim_{i\to+\infty} \mathbf{q}_c[i] = \lim_{i\to+\infty} \bar{\mathbf{q}}_c[i] = \mathbf{q}_c^{\text{opt}}$, with $\mathbf{V}^{\text{opt}}, \mathbf{p}_c^{\text{opt}}, \mathbf{q}_c^{\text{opt}}$ denoting the optimal solutions of the OID problems (4) and (5). □

Notice that problem (12) can be conveniently reformulated in a standard SDP form (which involves the minimization of a linear function, subject to linear (in) equalities and linear matrix inequalities) by introducing pertinent auxiliary optimization variables and by using the Schur complement [11], [27], [30]. Finally, for a given consensus error $0 < \epsilon \ll 1$, the algorithm terminates when $\|\bar{\mathbf{p}}_c[i] - \mathbf{p}_c[i]\|_2^2 + \|\bar{\mathbf{q}}_c[i] - \mathbf{q}_c[i]\|_2^2 \leq \epsilon$. However, it is worth emphasizing that, at each iteration i, the utility company solves a consensus-enforcing regularized OID problem, which yields intermediate voltages and power flows that clearly adhere to electrical network constraints.

Once the decentralized algorithm has converged, the real and reactive setpoints are implemented in the PV inverters. Notice, however, that Algorithm 1 affords an *online* implementation, that is, the intermediate PV inverter setpoints $\bar{\mathbf{p}}_c[i], \bar{\mathbf{q}}_c[i]$ are dispatched (and set at the customer side) as and when they become available, rather than waiting for the algorithm to converge.

IV. DOID: Network Cluster Partitions

Consider the case where the distribution network is partitioned into clusters, with $\mathcal{C}^a \subset \mathcal{N}$ denoting the set of nodes within cluster a. Also, define $\tilde{\mathcal{C}}^a := \mathcal{C}^a \cup \{n | (m,n) \in \mathcal{E}, m \in \mathcal{C}^a, n \in \mathcal{C}^j, a \neq j\}$; that is, $\tilde{\mathcal{C}}^a$ also includes the nodes belonging to different clusters that are connected to the ath one by a distribution line [12], [23] (see Fig. 5 for an illustration). Hereafter, superscript $(\cdot)^a$ will be used to specify quantities pertaining to cluster a; e.g., $\mathcal{H}^a$ is the set of houses located within cluster $\mathcal{C}^a$, and vectors $\bar{\mathbf{p}}_c^a, \bar{\mathbf{q}}_c^a$ collect copies of the setpoints of PV inverters $h \in \mathcal{H}^a$ available with the ath CEM [cf., (5)]. With regard to notation, an exception is $\mathbf{V}^a$, which denotes the submatrix of $\mathbf{V}$ corresponding to nodes in the extended cluster $\tilde{\mathcal{C}}^a$.

Based on this network partitioning, consider decoupling the network-related cost $\bar{C}(\mathbf{V}, \bar{\mathbf{p}}_c, \bar{\mathbf{q}}_c)$ in (5a) as

$$\bar{C}(\mathbf{V}, \bar{\mathbf{p}}_c, \bar{\mathbf{q}}_c) = \sum_{a=1}^{N_a} \underbrace{\left[C^a(\mathbf{V}^a, \bar{\mathbf{p}}_c^a) + \lambda^a \sum_{h \in \mathcal{H}^a} \|[\bar{P}_{c,h}, \bar{Q}_{c,h}]\|_2 \right]}_{:= \bar{C}^a(\mathbf{V}^a, \bar{\mathbf{p}}_c^a, \bar{\mathbf{q}}_c^a)}$$

where N_a is the number of clusters, $C^a(\mathbf{V}^a, \bar{\mathbf{p}}_c^a)$ captures optimization objectives of the ath cluster (e.g., power losses within the cluster [12], [17]), and the sparsity-promoting regularization function is used to determine which PV inverters in $\mathcal{H}^a$ provide ancillary services. Further, per cluster $a = 1, \ldots, N_a$ define the region of feasible power flows as [cf., (5b)–(5e)]

$$\mathcal{R}^a := \left\{ \mathbf{V}^a, \bar{\mathbf{p}}_c^a, \bar{\mathbf{q}}_c^a : \begin{array}{l} \mathrm{Tr}(\mathbf{A}_h^a \mathbf{V}^a) = \bar{P}_h - \bar{P}_{c,h}, \quad \forall h \in \mathcal{H}^a \\ \mathrm{Tr}(\mathbf{B}_h^a \mathbf{V}^a) = -Q_{\ell,h} + \bar{Q}_{c,h}, \forall h \in \mathcal{H}^a \\ \mathrm{Tr}(\mathbf{A}_n^a \mathbf{V}^a) = 0, \forall n \in \mathcal{U}^a \\ \mathrm{Tr}(\mathbf{B}_n^a \mathbf{V}^a) = 0, \forall n \in \mathcal{U}^a \\ V_{\min}^2 \leq \mathrm{Tr}(\mathbf{M}_n^a \mathbf{V}^a) \leq V_{\max}^2, \forall n \in \mathcal{C}^a \end{array} \right\}$$

where $\mathbf{A}_h^a, \mathbf{B}_h^a$, and $\mathbf{M}_h^a$ are the submatrices of $\mathbf{A}_h, \mathbf{B}_h$, and $\mathbf{M}_h$, respectively, formed by extracting rows and columns corresponding to nodes in $\tilde{\mathcal{C}}^a$. With these definitions, problem (5) can be equivalently formulated as

$$\min_{\substack{\mathbf{V}, \mathbf{p}_c, \mathbf{q}_c \\ \bar{\mathbf{p}}_c, \bar{\mathbf{q}}_c}} \sum_a \left[\bar{C}^a(\mathbf{V}^a, \bar{\mathbf{p}}_c^a, \bar{\mathbf{q}}_c^a) + \sum_{h \in \mathcal{H}^a} R_h(P_{c,h}) \right] \quad (15a)$$

$$\text{s. to } \mathbf{V} \succeq \mathbf{0}, \text{ and}$$

$$\{\mathbf{V}^a, \bar{\mathbf{p}}_c^a, \bar{\mathbf{q}}_c^a\} \in \mathcal{R}^a \qquad \forall a \quad (15b)$$

$$(P_{c,h}, Q_{c,h}) \in \mathcal{F}_h^{\mathrm{OID}} \qquad \forall h \in \mathcal{H}^a, \forall a \quad (15c)$$

$$\bar{P}_{c,h} = P_{c,h}, \; \bar{Q}_{c,h} = Q_{c,h} \quad \forall h \in \mathcal{H}^a, \forall a. \quad (15d)$$

Notice that, similar to (5g), constraints (15d) ensure that the CEM and customer-owned PV systems consent on the optimal PV inverter setpoints. Formulation (15) effectively decouples cost, power flow constraints, and PV-related consensus constraints (15d) on a per-cluster basis. The main challenge toward solving (15) in a decentralized fashion lies in the positive-semidefinite (PSD) constraint $\mathbf{V} \succeq \mathbf{0}$, which clearly couples the matrices $\{\mathbf{V}^a\}$. To address this challenge, results on completing partial Hermitian matrices from [31] will be leveraged to identify partitions of the distribution network in clusters for which the PSD constraint on $\mathbf{V}$ would decouple to $\mathbf{V}^a \succeq \mathbf{0}$, $\forall a$. This decoupling would clearly facilitate the decomposability of (15) in per-cluster subproblems [12], [23].

Toward this end, first define the set of *neighboring clusters* for the ath one as $\tilde{\mathcal{B}}^a := \{j | \tilde{\mathcal{C}}^a \cap \tilde{\mathcal{C}}^j \neq 0\}$. Further, let $\mathcal{G}_\mathcal{C}$ be a graph capturing the control architecture of the distribution network, where nodes represent the clusters and edges connect neighboring clusters (i.e., based on sets $\{\tilde{\mathcal{B}}^a\}$); for example, the graph $\mathcal{G}_\mathcal{C}$ associated with the network in Fig. 5 has two nodes, connected through an edge (since the two areas are connected). In general, it is clear that if clusters a and j are neighbors, then CEM a and CEM j must agree on the voltages at the two end points of the distribution line connecting the two clusters. For example, with reference to Fig. 5, notice that line $(8, 11)$ connects clusters 1 and 2. Therefore, CEM 1 and CEM 2 must agree on voltages V_8 and V_{11}. Finally, let $\mathbf{V}_j^a$ denote the submatrix of $\mathbf{V}^a$ corresponding to the two voltages on the line connecting clusters a and j. Recalling the previous example, agreeing on V_8 and V_{11} is tantamount to setting $\mathbf{V}_2^1 = \mathbf{V}_1^2$, where $\mathbf{V}_2^1$ is a 2×2 matrix representing the outer-product $[V_8, V_{11}]^{\mathrm{T}}[V_8, V_{11}]^*$. Using these definitions, the following proposition can be proved by suitably adapting the results of [12] and [23] to the problem at hand.

Proposition 2: Suppose: 1) the cluster graph $\mathcal{G}_\mathcal{C}$ is a tree, and 2) clusters are not nested (i.e., $|\tilde{\mathcal{C}}^a \backslash (\tilde{\mathcal{C}}^a \bigcap \tilde{\mathcal{C}}^j)| > 0 \, \forall a \neq j$). Then, (15a) is equivalent to the following problem:

$$\min_{\substack{\{\mathbf{V}^a, \mathbf{p}_c^a, \mathbf{q}_c^a\} \\ \bar{\mathbf{p}}_c, \bar{\mathbf{q}}_c}} \sum_a \left[\bar{C}^a(\mathbf{V}^a, \bar{\mathbf{p}}_c^a, \bar{\mathbf{q}}_c^a) + \sum_{h \in \mathcal{H}^a} R_h(P_{c,h}) \right] \quad (16a)$$

$$\text{s. to (15b)–(15d) and}$$

$$\mathbf{V}^a \succeq \mathbf{0} \qquad \forall a \quad (16b)$$

$$\mathbf{V}_j^a = \mathbf{V}_a^j, \quad \forall j \in \tilde{\mathcal{B}}^a \quad \forall a. \quad (16c)$$

Under 1 and 2, there exists a rank-1 matrix $\mathbf{V}^{\mathrm{opt}}$ solving (15) optimally if and only if $\mathrm{rank}\{\mathbf{V}^a\} = 1, \forall a = 1, \ldots, N_a$. □

Notice that the $|\mathcal{N}| \times |\mathcal{N}|$ matrix $\mathbf{V}$ is replaced by per-cluster reduced-dimensional $|\tilde{\mathcal{C}}^a| \times |\tilde{\mathcal{C}}^a|$ matrices $\{\mathbf{V}^a\}$ in (16). Proposition 2 is grounded on the results of [31], which asserts that a PSD matrix $\mathbf{V}$ can be obtained starting from submatrices $\{\mathbf{V}^a\}$ if and only if the graph induced by $\{\mathbf{V}^a\}$ is chordal. Since a PSD matrix can be reconstructed from $\{\mathbf{V}^a\}$, it suffices to impose contraints $\mathbf{V}^a \succeq \mathbf{0}$, $\forall a = 1, \ldots, N_a$. Assumptions 1 and 2 provide sufficient conditions for the graph induced by $\{\mathbf{V}^a\}$ to be chordal, and they are typically satisfied in practice (e.g., when each cluster is set to be a lateral or a sublateral). The second part of the proposition asserts that, for the completable PSD matrix $\mathbf{V}$ to have rank 1, all matrices $\mathbf{V}^a$ must have rank 1; thus, if $\mathrm{rank}\{\mathbf{V}^a\} = 1$ for all clusters, then $\{\mathbf{V}^a\}$ represents a globally optimal solution for given inverter setpoints.

Similar to (6), auxiliary variables are introduced to enable decomposability of (16) in per-cluster subproblems. With variables x_h, y_h associated with inverter h, and $\mathbf{W}^{a,j}, \mathbf{Q}^{a,j}$ with neighboring clusters a and j, (16) is reformulated as

$$\min_{\substack{\{\mathbf{V}^a, \mathbf{p}_c^a, \mathbf{q}_c^a\} \\ \bar{\mathbf{p}}_c^a, \bar{\mathbf{q}}_c^a \\ \{\mathbf{W}^{a,j}, \mathbf{Q}^{a,j}, x_h, y_h\}}} \sum_a \left[\bar{C}^a(\mathbf{V}^a, \bar{\mathbf{p}}_c^a, \bar{\mathbf{q}}_c^a) + \sum_{h \in \mathcal{H}^a} R_h(P_{c,h}) \right]$$

$$\text{s. to (15b)–(15c)}, \mathbf{V}^{\mathrm{a}} \succeq \mathbf{0} \quad \forall \mathrm{a}, \text{ and}$$

$$\Re\{\mathbf{V}_j^a\} = \mathbf{W}^{a,j}, \ \mathbf{W}^{a,j} = \mathbf{W}^{j,a} \quad \forall j \in \tilde{\mathcal{B}}^a, \quad \forall a \quad (17a)$$

$$\Im\{\mathbf{V}_j^a\} = \mathbf{Q}^{a,j}, \quad \mathbf{Q}^{a,j} = \mathbf{Q}^{j,a}, \quad \forall j \in \tilde{\mathcal{B}}^a, \quad \forall a \quad (17b)$$

$$\bar{P}_{c,h} = x_h, \quad x_h = P_{c,h} \quad \forall h \in \mathcal{H}^a, \quad \forall a \quad (17c)$$

$$\bar{Q}_{c,h} = y_h, \quad y_h = Q_{c,h} \quad \forall h \in \mathcal{H}^a, \quad \forall a. \quad (17d)$$

This problem can be solved across clusters by resorting to ADMM. To this end, a partial quadratically augmented Lagrangian, obtained by dualizing constraints $\Re\{\mathbf{V}_j^a\} = \mathbf{W}^{a,j}$, $\Im\{\mathbf{V}_j^a\} = \mathbf{Q}^{a,j}$, $\bar{P}_{c,h} = x_h$, and $\bar{Q}_{c,h} = y_h$ is defined first; then, the standard ADMM steps involve a cyclic minimization of the resultant Lagrangian with respect to $\{\mathbf{V}^a, \mathbf{p}_c^a, \mathbf{q}_c^a, \bar{\mathbf{p}}_c^a, \bar{\mathbf{q}}_c^a\}$ (by keeping the remaining variables fixed); the auxiliary variables $\{\mathbf{W}^{a,j}, \mathbf{Q}^{a,j}, x_h, y_h\}$; and, finally, a dual ascent step [15, Sec. 3.4]. It turns out that Lemma 1 still holds in the present case. Thus, using this lemma, along with the result in [12, Lemma 3], it can be shown that the ADMM steps can be simplified as described next (the derivation is omitted due to space limitations):

[S1″] Each PV system updates the local copy $\mathcal{P}_h[i+1]$ via (13), while each CEM updates the voltage profile of its cluster and the local copies of the setpoints of inverters $\mathcal{H}^a$ by solving the following convex problem:

$$\bar{\mathcal{P}}^a[i+1] := \arg \min_{\substack{\mathbf{V}^a, \bar{\mathbf{p}}_c^a, \bar{\mathbf{q}}_c^a \\ \{\alpha_j \geq 0, \beta_j \geq 0\}}} \Big[\bar{C}^a(\mathbf{V}^a, \bar{\mathbf{p}}_c^a, \bar{\mathbf{q}}_c^a) + F^a(\bar{\mathbf{p}}_c^a, \bar{\mathbf{q}}_c^a, \{\mathcal{P}_h[i]\}) + F_V^a(\mathbf{V}^a, \{\mathbf{V}^j[i]\}) \Big] \quad (18a)$$

$$\text{s. to } \{\mathbf{V}^a, \bar{\mathbf{p}}_c^a, \bar{\mathbf{q}}_c^a\} \in \mathcal{R}^a, \mathbf{V}^a \succeq \mathbf{0}, \text{ and} \quad (18b)$$

$$\begin{bmatrix} -\alpha_j & \mathbf{a}_j^{\mathrm{T}} \\ \mathbf{a}_j & -\mathbf{I} \end{bmatrix} \preceq \mathbf{0}, \quad \forall j \in \tilde{\mathcal{B}}^a \quad (18c)$$

$$\begin{bmatrix} -\beta_j & \mathbf{b}_j^{\mathrm{T}} \\ \mathbf{b}_j & -\mathbf{I} \end{bmatrix} \preceq \mathbf{0}, \quad \forall j \in \tilde{\mathcal{B}}^a \quad (18d)$$

where vectors $\mathbf{a}_j$ and $\mathbf{b}_j$ collect the real and imaginary parts, respectively, of the entries of the matrix $\mathbf{V}_j^a - \frac{1}{2}\left(\mathbf{V}_j^a[i] + \mathbf{V}_a^j[i]\right)$; the regularization function $F^a(\bar{\mathbf{p}}_c^a, \bar{\mathbf{q}}_c^a, \{\mathcal{P}_h[i]\})$ enforcing consensus on the inverter setpoints is defined as in (12b) (but with the summation limited to inverters $\mathcal{H}^a$), and $F_V(\mathbf{V}^a, \{\mathbf{V}^j[i]\})$ is given by

$$F_V^a(\mathbf{V}^a, \{\mathbf{V}^j[i]\}) := \sum_{j \in \tilde{\mathcal{B}}^a} \Big[\frac{\kappa}{2}(\alpha_j + \beta_j) + \mathrm{Tr}(\boldsymbol{\Upsilon}_{a,i}^{\mathrm{T}}[i] \Re\{\mathbf{V}_j^a\}) + \mathrm{Tr}(\boldsymbol{\Psi}_{a,i}^{\mathrm{T}}[i] \Im\{\mathbf{V}_j^a\}) \Big]. \quad (18e)$$

[S2″] Update dual variables $\{\gamma_h, \mu_h\}$ via (14a) at both the customer and the CEMs; variables $\{\boldsymbol{\Upsilon}_{a,i}, \boldsymbol{\Psi}_{a,i}\}$ are updated locally per cluster $a = 1, \ldots, N_a$ as

$$\boldsymbol{\Upsilon}_{a,j}[i+1] = \boldsymbol{\Upsilon}_{a,j}[i] + \frac{\kappa}{2}\left(\Re\{\mathbf{V}_j^a[i+1]\} - \Re\{\mathbf{V}_a^j[i+1]\}\right) \quad (19a)$$

$$\boldsymbol{\Psi}_{a,j}[i+1] = \boldsymbol{\Psi}_{a,j}[i] + \frac{\kappa}{2}\left(\Im\{\mathbf{V}_j^a[i+1]\} - \Im\{\mathbf{V}_a^j[i+1]\}\right). \quad (19b)$$

Algorithm 2 DOID: Multicluster distributed optimization.

Set $\gamma_h[0] = \mu_h[0] = 0$ for all $h \in \mathcal{H}^a$ and for all clusters.
Set $\boldsymbol{\Upsilon}_{a,j}[0] = \boldsymbol{\Psi}_{a,j}[0] = \mathbf{0}$ for all pair of neighboring clusters.
for $i = 1, 2, \ldots$ (repeat until convergence) **do**
1. **[CEM-a]**: update $\mathbf{V}^a[i+1]$ and $\bar{\mathbf{p}}_c^a, \bar{\mathbf{q}}_c^a$ via (18).
   [Customer-h]: update $\bar{P}_{c,h}[i+1], \bar{Q}_{c,h}[i+1]$ via (13).
2. **[CEM-a]**: send $\mathbf{V}_j^a[i+1]$ to CEM j;
   [CEM-a]: receive $\mathbf{V}_a^j[i+1]$ from CEM j; repeat $\forall j \in \tilde{\mathcal{B}}^a$
3. **[CEM-a]**: send $\bar{P}_{c,h}[i+1], \bar{Q}_{c,h}[i+1]$ to EMU-h; repeat for all $h \in \mathcal{H}^a$.
   [Customer-h]: receive $\bar{P}_{c,h}[i+1], \bar{Q}_{c,h}[i+1]$ from CEM a; send $P_{c,h}[i+1], Q_{c,h}[i+1]$ to CEM a; repeat for all $h \in \mathcal{H}^a$.
   [CEM-a]: receive $P_{c,h}[i+1], Q_{c,h}[i+1]$ from h; repeat for all $h \in \mathcal{H}^a$.
4. **[CEM-a]**: update $\{\gamma_h[i+1], \mu_h[i+1]\}_{h \in \mathcal{H}}$ via (14).
   [CEM-a]: update $\{\boldsymbol{\Upsilon}_{a,j}[i+1], \boldsymbol{\Psi}_{a,j}[i+1]\}$ via (19);
   [Customer-h]: update dual variables $\gamma_h[i+1], \mu_h[i+1]$ via (14);

end for
Implement setpoints in the PV inverters.

The resultant decentralized algorithm is tabulated as Algorithm 2, illustrated in Fig. 5, and it involves an exchange of: 1) the local submatrices $\{\mathbf{V}_j^a[i+1]\}$ among neighboring CEMs to agree upon the voltages on lines connecting clusters; and 2) the local copies of the PV inverter setpoints between the CEM and customer-owned PV systems. Using arguments similar to Proposition 3, convergence of the algorithm can be readily established.

Proposition 3: For any $\kappa > 0$, the iterates $\{\bar{\mathcal{P}}^a[i]\}$, $\{\mathcal{P}_h[i]\}, \mathcal{D}[i]$ produced by **[S1″]–[S2″]** are convergent, and they converge to a solution of the OID problems (4) and (15). □

Once the decentralized algorithm has converged, the real and reactive setpoints are implemented by the PV inverter controllers.

Finally, notice that the worst-case complexity of an SDP is on the order $\mathcal{O}(\max\{N_c, N_v\}^4 \sqrt{N_v} \log(1/\epsilon))$ for general purpose solvers, with N_c denoting the total number of constraints, N_v the total number of variables, and $\epsilon > 0$ a given solution accuracy [30]. It follows that the worst-case complexity of (18) is markedly lower than the one of the centralized problem (4). Further, the sparsity of $\{\mathbf{A}_n, \mathbf{B}_n, \mathbf{M}_n\}$ and the so-called chordal structure of the underlying electrical graph matrix can be exploited to obtain substantial computational savings (see, e.g., [32]).

V. Case Studies

Consider the distribution network in Fig. 1, which is adopted from [8] and [11]. The simulation parameters are set as in [11] to check the consistency between the results of centralized and decentralized schemes. Specifically, the pole–pole distance is

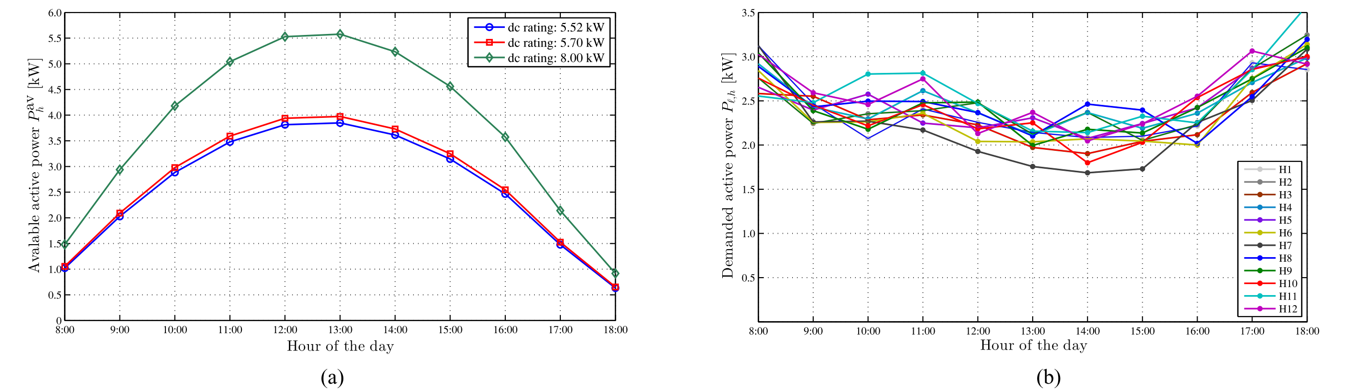

Fig. 6. Problem inputs. (a) Available active powers $\{P_h \text{av}\}$ from inverters with dc ratings of 5.52, 5.70, and 8.00 kW. (b) Demanded active loads at the households (reactive demand is computed by presuming a power factor of 0.9).

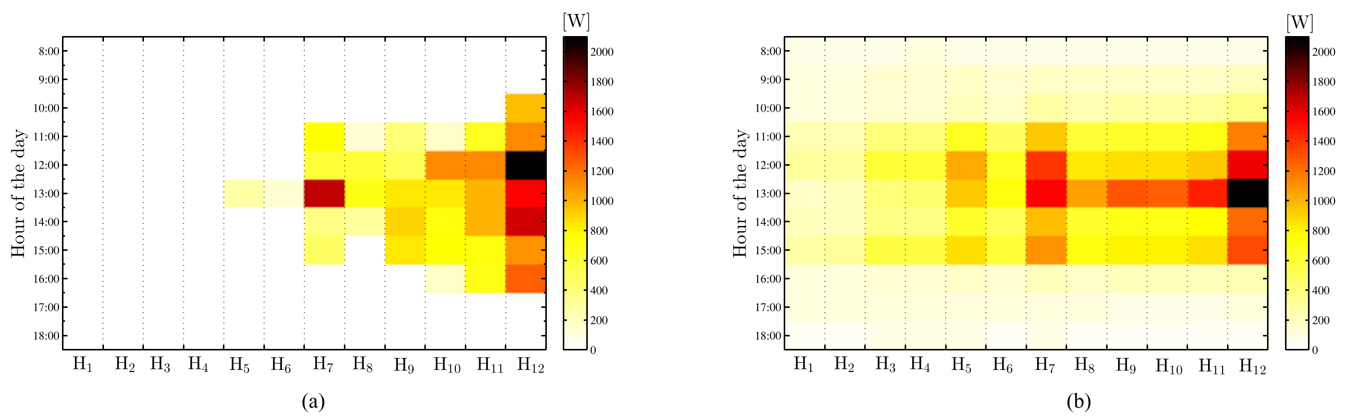

Fig. 7. Solution of the centralized OID problem (4a): Curtailed active power per each household for (a) $\lambda = 0.8$ and (b) $\lambda = 0$ (see also [11]).

set to 50 m, lengths of the drop lines are set to 20 m, and voltage limits $V^{\min}, V^{\max}$ are set to 0.917 and 1.042 p.u., respectively (see, e.g., [8]). The optimization package CVX[1] is employed to solve relevant optimization problems in MATLAB. In all the conducted numerical tests, the rank of matrices $\mathbf{V}$ and $\{\mathbf{V}^a\}$ was always 1, meaning that globally optimal solutions were obtained for given inverter setpoints.

The available active powers $\{P_h^{\text{av}}\}_{h\in\mathcal{H}}$ are computed using the System Advisor Model[2] of the National Renewable Energy Laboratory; specifically, the typical meteorological year data for Minneapolis, MN, USA, during the month of July are used. All 12 houses feature fixed roof-top PV systems, with a dc–ac derating coefficient of 0.77. The dc ratings of the houses are as follows: 5.52 kW for houses $\text{H}_1, \text{H}_9, \text{H}_{10}$; 5.70 kW for $\text{H}_2, \text{H}_6, \text{H}_8, \text{H}_{11}$; and 8.00 kW for the remaining five houses. The active powers $\{P_h^{\text{av}}\}$ generated by the inverters with dc ratings of 5.52, 5.70, and 8.00 kW are plotted in Fig. 6(a). As suggested in [3], it is assumed that the PV inverters are oversized by 10% of the resultant ac rating. The minimum power factor for the inverters is set to 0.85 [33].

[1][Online] Available: `http://cvxr.com/cvx/`
[2][Online] Available at `https://sam.nrel.gov/`

The residential load profile is obtained from the Open Energy Info database, and the base load experienced in downtown Saint Paul, MN, USA, during the month of July is used for this test case. To generate 12 different load profiles, the base active power profile is perturbed using a Gaussian random variable with zero mean and standard deviation 200 W; the resultant active loads $\{P_{\ell,h}\}$ are plotted in Fig. 6(b). To compute the reactive loads $\{Q_{\ell,h}\}$, a power factor of 0.9 is presumed [8].

Assume that the objective of the utility company is to minimize the power losses in the network; that is, upon defining the symmetric matrix $\mathbf{L}_{mn} := \Re\{y_{mn}\}(\mathbf{e}_m - \mathbf{e}_n)(\mathbf{e}_m - \mathbf{e}_n)^{\text{T}}$ per distribution line $(m, n) \in \mathcal{E}$, function $C_{\text{utility}}(\mathbf{V}, \bar{\mathbf{p}}_c)$ is set to $C_{\text{utility}}(\mathbf{V}, \bar{\mathbf{p}}_c) = \text{Tr}(\mathbf{LV})$, with $\mathbf{L} := \sum_{(m,n)\in\mathcal{E}} \mathbf{L}_{mn}$ (see [11] for more details). At the customer side, function $R_h(P_{c,h})$ is set to $R_h(P_{c,h}) = 0.1 P_{c,h}$. The impact of varying the parameter λ is investigated in detail in [11] and further illustrated in Fig. 7, where the solution of the centralized OID problem (4a) is reported for different values of the parameter λ [cf., (3)]. Specifically, Fig. 7(a) illustrates the active power curtailed from each inverter during the course of the day when $\lambda = 0.8$, whereas the result in Fig. 7(b) was obtained by setting $\lambda = 0$. It is clearly seen that in the second case all inverters

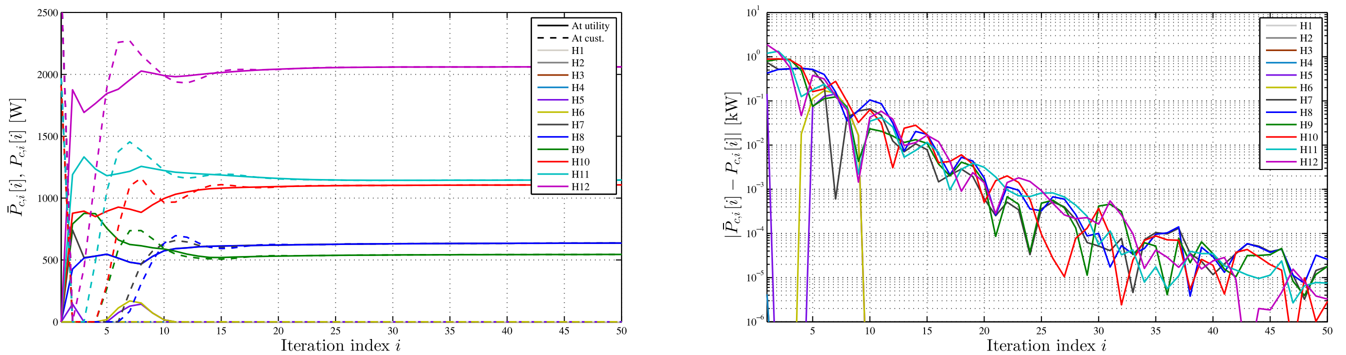

(a) (b)

Fig. 8. Convergence of Algorithm 1. (a) Values of $\{P_{c,h}[i]\}_{h\in\mathcal{H}}$ (dashed lines) and $\{\bar{P}_{c,h}[i]\}_{h\in\mathcal{H}}$ as a function of the ADMM iteration index i. (b) Consensus error $|P_{c,h}[i] - \bar{P}_{c,h}[i]|$, for all houses $h \in \mathcal{H}$ as a function of i.

are controlled; in fact, they all curtail active power from 8:00 to 18:00. When $\lambda = 0.8$, the OID seeks a tradeoff between achievable objective and number of controlled inverters. It is clearly seen that the number of participating inverters grows with increasing solar irradiation, with a maximum of seven inverters operating away from the business-as-usual point at 13:00.

The convergence of Algorithm 1 is showcased for $\lambda = 0.8$, $C_{\text{utility}}(\mathbf{V}, \bar{\mathbf{p}}_c) = \text{Tr}(\mathbf{LV})$, and $R_h(P_{c,h}) = 0.1P_{c,h}$, and by utilizing the solar irradiation conditions at 12:00. Fig. 8(a) depicts the trajectories of the iterates $\{P_{c,h}[i]\}_{h\in\mathcal{H}}$ (dashed lines) and $\{\bar{P}_{c,h}[i]\}_{h\in\mathcal{H}}$ (solid lines) for all the houses H_1–H_{12}. The results match the ones in Fig. 7(a); in fact, at convergence (i.e., for iterations $i \geq 20$), only inverters at houses H_7–H_{12} are controlled, and the APC setpoints are in agreement. This result is expected, since problems (4) and (5) are *equivalent*; the only difference is that (4) affords only in centralized solution, whereas (5) is in a form that is suitable for the application of the ADMM to derive distributed solution schemes; see also [16], [29], and [34]. Finally, the trajectories of the setpoint consensus error $|P_{c,h}[i] - \bar{P}_{c,h}[i]|$, as a function of the ADMM iteration index i are depicted in Fig. 8(b). It can be clearly seen that the algorithm converges fast to a setpoint that is convenient for both utility and customers. Similar trajectories were obtained for the reactive power setpoints.

Fig. 9 represents the discrepancies between local voltages on the line $(8, 11)$; specifically, the trajectories of the voltage errors $|V_8^1[i] - V_8^2[i]|$ and $|V_{11}^1[i] - V_{11}^2[i]|$ are reported as a function of the ADMM iteration index i. The results indicate that the two CEMs consent on the voltage of the branch that connects the two clusters. The "bumpy" trend is typical of the ADMM (see, e.g., [29] and [34]). Similar trajectories were obtained for the inverter setpoints.

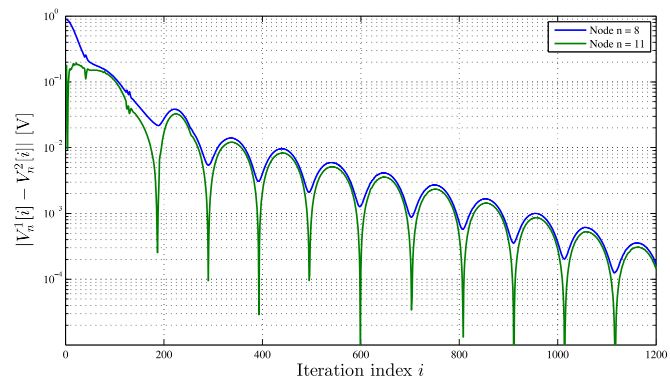

Fig. 9. Convergence of Algorithm 2: consensus error $|V_8^1[i] - V_8^2[i]|$ and $|V_{11}^1[i] - V_{11}^2[i]|$ as a function of the ADMM iteration index i.

VI. Concluding Remarks

A suite of decentralized approaches for computing optimal real and reactive power setpoints for residential PV inverters were developed. The proposed decentralized OID strategy offers a comprehensive framework to share computational burden and optimization objectives across the distribution network, while highlighting future business models that will enable customers to actively participate in distribution-system markets.

References

[1] E. Liu, and J. Bebic, "Distribution system voltage performance analysis for high-penetration photovoltaics," (Technical Monitor: B. Kroposki), Nat. Renewable Energy Lab., Golden, CO, USA, Subcontract Rep. NREL/SR-581-42298, Feb. 2008.

[2] E. Ntakou and M. C. Caramanis, "Price discovery in dynamic power markets with low-voltage distribution-network participants," presented at the IEEE PES Transmission and Distribution Conference, Chicago, IL, USA, 2014.

[3] K. Turitsyn, P. Súlc, S. Backhaus, and M. Chertkov, "Options for control of reactive power by distributed photovoltaic generators," *Proc. IEEE*, vol. 99, no. 6, pp. 1063–1073, Jun. 2011.

[4] P. Súlc, S. Backhaus, and M. Chertkov. (2013). Optimal distributed control of reactive power via the alternating direction method of multipliers. [Online]. Available at: http://arxiv.org/pdf/1310.5748v1.pdf

[5] P. Jahangiri and D. C. Aliprantis, "Distributed Volt/VAr control by PV inverters," *IEEE Trans. Power Syst.*, vol. 28, no. 3, pp. 3429–3439, Aug. 2013.

[6] M. Farivar, R. Neal, C. Clarke, and S. Low, "Optimal inverter VAR control in distribution systems with high PV penetration," presented at the IEEE PES General Meeting, San Diego, CA, USA, Jul. 2012.

[7] S. Bolognani and S. Zampieri, "A distributed control strategy for reactive power compensation in smart microgrids," *IEEE Trans. Autom. Control*, vol. 58, no. 11, pp. 2818–2833, Nov. 2013.

[8] R. Tonkoski, L. A. C. Lopes, and T. H. M. El-Fouly, "Coordinated active power curtailment of grid connected PV inverters for overvoltage prevention," *IEEE Trans. Sustain. Energy*, vol. 2, no. 2, pp. 139–147, Apr. 2011.

[9] A. Samadi, R. Eriksson, L. Soder, B. G. Rawn, and J. C. Boemer, "Coordinated active power-dependent voltage regulation in distribution grids with PV systems," *IEEE Trans. Power Del.*, vol. 29, no. 3, pp. 1454–1464, Jun. 2014.
[10] W. H. Kersting, *Distribution System Modeling and Analysis*, 2nd ed. Boca Raton, FL, USA: CRC Press, 2007.
[11] E. Dall'Anese, S. V. Dhople, and G. B. Giannakis, "Optimal dispatch of photovoltaic inverters in residential distribution systems," *IEEE Trans. Sustain. Energy*, vol. 5, no. 2, pp. 487–497, Apr. 2014.
[12] E. Dall'Anese, H. Zhu, and G. B. Giannakis, "Distributed optimal power flow for smart microgrids," *IEEE Trans. Smart Grid*, vol. 4, no. 3, pp. 1464–1475, Sep. 2013.
[13] P. Samadi, A. H. Mohsenian-Rad, R. Schober, V. Wong, and J. Jatskevich, "Optimal real-time pricing algorithm based on utility maximization for smart grid," presented at the IEEE International Conference on Smart Grid Communications, Gaithersburg, MD, USA, 2010.
[14] N. Gatsis and G. B. Giannakis, "Residential load control: Distributed scheduling and convergence with lost AMI messages," *IEEE Trans. Smart Grid*, vol. 3, no. 2, pp. 770–786, Jun. 2012.
[15] D. P. Bertsekas, and J. N. Tsitsiklis, *Parallel and Distributed Computation: Numerical Methods*. Englewood Cliffs, NJ, USA: Prentice-Hall, 1989.
[16] S. Boyd, N. Parikh, E. Chu, B. Peleato, and J. Eckstein, "Distributed optimization and statistical learning via the alternating direction method of multipliers," *Found. Trends Mach. Learn.*, vol. 3, pp. 1–122, 2011.
[17] R. Baldick, B. H. Kim, C. Chase, and Y. Luo, "A fast distributed implementation of optimal power flow," *IEEE Trans. Power Syst.*, vol. 14, no. 3, pp. 858–864, Aug. 1999.
[18] F. J. Nogales, F. J. Prieto, and A. J. Conejo, "A decomposition methodology applied to the multi-area optimal power flow problem," *Ann. Oper. Res.*, no. 120, pp. 99–116, 2003.
[19] G. Hug-Glanzmann and G. Andersson, "Decentralized optimal power flow control for overlapping areas in power systems," *IEEE Trans. Power Syst.*, vol. 24, no. 1, pp. 327–336, Feb. 2009.
[20] T. Erseghe, "Distributed optimal power flow using ADMM," *IEEE Trans. Power Syst.*, vol. 29, no. 5, pp. 2370–2380, Sep. 2014.
[21] S. Magnusson, P. C. Weeraddana, and C. Fischione. (2014 Jan.). A distributed approach for the optimal power flow problem based on ADMM and sequential convex approximations. [Online]. Available at: http://arxiv.org/abs/1401.4621
[22] A. Y. Lam, B. Zhang, A. Domínguez-García, and D. Tse. (2012). Optimal distributed voltage regulation in power distribution networks. [Online]. Available at http://arxiv.org/abs/1204.5226v1
[23] H. Zhu and G. B. Giannakis, "Multi-area state estimation using distributed SDP for nonlinear power systems," presented at the 3rd International Conference on Smart Grid Communications, Tainan City, Taiwan, Nov. 2012.
[24] V. Kekatos, and G. B. Giannakis, "Distributed robust power system state estimation," *IEEE Trans. Power Syst.*, vol. 28, no. 2, pp. 1617–1626, May 2013.
[25] E. Dall'Anese and G. B. Giannakis, "Risk-constrained microgrid reconfiguration using group sparsity," *IEEE Trans. Sustain. Energy,* vol. 5, no. 4, pp. 1415–1425, Oct. 2014.
[26] A. T. Puig, A. Wiesel, G. Fleury, and A. O. Hero, "Multidimensional shrinkage-thresholding operator and group LASSO penalties," *IEEE Signal Process. Lett.*, vol. 18, no. 6, pp. 363–366, Jun. 2011.
[27] J. Lavaei and S. H. Low, "Zero duality gap in optimal power flow problem," *IEEE Trans. Power Syst.*, vol. 27, no. 1, pp. 92–107, Feb. 2012.
[28] J. Lavaei, D. Tse, and B. Zhang, "Geometry of power flows and optimization in distribution networks," presented at the IEEE PES General Meeting, San Diego, CA, USA, 2012.
[29] T. Erseghe, D. Zennaro, E. Dall'Anese, and L. Vangelista, "Fast consensus by the alternating direction multipliers method," *IEEE Trans. Signal Process.*, vol. 59, no. 11, pp. 5523–5537, Nov. 2011.
[30] L. Vandenberghe and S. Boyd, "Semidefinite programming," *SIAM Rev.*, vol. 38, no. 1, pp. 49–95, Mar. 1996.
[31] R. Grone, C. R. Johnson, E. M. Sá, and H. Wolkowicz, "Positive definite completions of partial Hermitian matrices," *Linear Algebra Appl.*, vol. 58, pp. 109–124, 1984.
[32] R. A. Jabr, "Exploiting sparsity in SDP relaxations of the OPF problem," *IEEE Trans. Power Syst.*, vol. 2, no. 27, pp. 1138–1139, May 2012.
[33] M. Braun, J. Künschner, T. Stetz, and B. Engel, "Cost optimal sizing of photovoltaic inverters—Influence of new grid codes and cost reductions," presented at the 25th European Photovoltaic Solar Energy Conference and Exhibition, Valencia, Spain, Sep. 2010.
[34] H. Zhu, G. B. Giannakis, and A. Cano, "Distributed in-network channel decoding," *IEEE Trans. Signal Process.*, vol. 57, no. 10, pp. 3970–3983, Oct. 2009.

Emiliano Dall'Anese (S'08–M'11) received the Laurea Triennale (B.Sc.) degree and the Laurea Specialistica (M.Sc.) degree in telecommunications engineering from the University of Padova, Padova, Italy, in 2005 and 2007, respectively, and the Ph.D. degree in information engineering from the Department of Information Engineering, University of Padova, in 2011.

From January 2009 to September 2010, he was a Visiting Scholar with the Department of Electrical and Computer Engineering, University of Minnesota, Minneapolis, MN, USA. Since January 2011, he has been a Post-Doctoral Associate at the Department of Electrical and Computer Engineering and Digital Technology Center, University of Minnesota. His research interests include power systems, signal processing, optimization, and communications. Current research focuses on energy management in future power systems and grid informatics.

Sairaj V. Dhople (S'09–M'13) received the B.S., M.S., and Ph.D. degrees in electrical engineering from the University of Illinois at Urbana-Champaign, Champaign, IL, USA, in 2007, 2009, and 2012, respectively.

He is currently an Assistant Professor in the Department of Electrical and Computer Engineering, University of Minnesota, Minneapolis, MN, USA, where he is affiliated with the Power and Energy Systems Research Group. His research interests include modeling, analysis, and control of power electronics and power systems with a focus on renewable integration.

Brian B. Johnson (S'08–M'13) received the B.S. degree in physics from Texas State University, San Marcos, TX, USA, in 2008, and the M.S. and Ph.D. degrees in electrical and computer engineering from the University of Illinois at Urbana-Champaign, Champaign, IL, USA, in 2010 and 2013, respectively.

He is currently an Electrical Engineer with the National Renewable Energy Laboratory, Golden, CO, USA. His research interests are in power electronics, distributed generation, renewable energy systems, and controls.

Dr. Johnson received the National Science Foundation Graduate Research Fellowship in 2010.

Georgios B. Giannakis (F'97) received the Diploma degree in electrical engineering from the National Technical University of Athens, Athens, Greece, in 1981. He received the M.Sc. degree in electrical engineering, the M.Sc. degree in mathematics, and the Ph.D. degree in electrical engineering from the University of Southern California, Los Angeles, CA, USA, in 1983, 1986, 1986, respectively.

Since 1999, he has been a Professor with the University of Minnesota, Minneapolis, MN, USA, where he now holds an ADC Chair in Wireless Telecommunications in the Department of Electrical and Computer Engineering, and serves as the Director of the Digital Technology Center. His research interests include communications, networking, and statistical signal processing—subjects on which he has published more than 370 journal papers, 630 conference papers, 21 book chapters, two edited books, and two research monographs (h-index 109). Current research focuses on sparsity and big data analytics, wireless cognitive radios, mobile ad hoc networks, renewable energy, power grid, gene-regulatory, and social networks. He is the (co)inventor of 23 patents issued.

Dr. Giannakis received as (co)recipient of eight best paper awards from the IEEE Signal Processing (SP) and Communications Societies, including the G. Marconi Prize Paper Award in Wireless Communications. He also received technical achievement awards from the SP Society (2000) and from European Association for Signal Processing (EURASIP) (2005), a Young Faculty Teaching Award, the G. W. Taylor Award for Distinguished Research from the University of Minnesota, and the IEEE Fourier Technical Field Award (2014). He is a Fellow of EURASIP, and has served the IEEE in a number of posts, including that of a Distinguished Lecturer for the IEEE-SP Society.